CEAS Aeronautical Journal
https://doi.org/10.1007/s13272-025-00887-2

ORIGINAL PAPER

Reducing contrail formation by engine design and operating point adaptation of aircraft engines

Julian Callard[1] · Christian Klumpp[1] · Daniel Weintraub[1] · Stefan Henninger[1] · Peter Jeschke[1]

Received: 12 March 2025 / Revised: 16 July 2025 / Accepted: 7 August 2025
© The Author(s) 2025

Abstract

In this paper, we present an analysis of the effect of engine design modifications and operating point adaptation mechanisms on the conditions in the engine exhaust plume, with a focus on contrail formation which is evaluated using the Schmidt-Appleman criterion. Our goal is to find ways to prevent contrail formation and thus reduce the climate impact of aviation. We use the gas turbine performance software GasTurb to model an aircraft engine of a contemporary short- to medium-range aircraft. We then examine several operating point adaption mechanisms with regard to their influence on the exhaust conditions and the resulting mixing line in the Schmidt-Appleman diagram. These are the bypass and core nozzle areas, high- and low-pressure turbine capacities, a handling bleed, and a high-pressure bleed. The main influence on the mixing line in the Schmidt-Appleman diagram is the change in exhaust jet temperature and its water content, which is affected by the fuel flow resulting from the engine's operating point and efficiency. All measures are evaluated based on the shift in the critical altitude of contrail formation, with a minimum increase of 450 m in cruise flight conditions deemed necessary for any effective measure. We find that it is possible to reduce contrail formation. However, the critical altitude gains are only 57 m to 206 m for all measures investigated, which is insufficient to avoid contrail formation in practice, as calculated using the Schmidt-Appleman criterion. The measures also significantly increase specific fuel consumption, with more effective measures leading to higher increases of up to 35 %. Given the results presented, we find that engine operating point adaptations as examined in this paper are not suitable for contrail reduction due to their low effectiveness and significant increase in fuel consumption. More fundamental design changes, such as engine cycle adaptations or the use of hydrogen as a fuel, may offer greater potential for contrail reduction.

Keywords Contrail avoidance · Performance calculations · Climate impact reduction

Nomenclature

Roman letters

ALT	Altitude	m
EI	Emission index	-
FHV	Fuel heating value	$MJ\,kg^{-1}$
SFC	Specific fuel consumption	g/(kNs)
C_P	Specific heat capacity at constant pressure	$J\,kg^{-1}\,K^{-1}$
F_N	Net thrust	kN
G	Slope factor acc. to Eq. 1	$Pa\,K^{-1}$
h	Specific enthalpy	$J\,kg^{-1}$
M	Mach number	-
P_D	Partial pressure of water vapour	Pa
P_s	Static pressure	Pa
q	Water content	-
T	Total temperature	K
T_s	Static temperature	K
V	Velocity	ms^{-1}

✉ Julian Callard
callard@ist.rwth-aachen.de

Christian Klumpp
klumpp@ist.rwth-aachen.de

Daniel Weintraub
weintraub@ist.rwth-aachen.de

Stefan Henninger
henninger@ist.rwth-aachen.de

Peter Jeschke
jeschke@ist.rwth-aachen.de

[1] Institute of Jet Propulsion and Turbomachinery, RWTH Aachen University, Templergraben 55, 52062 Aachen, NRW, Germany

Published online: 08 September 2025

W	Mass flow	kg s^{-1}
OPR	Overall pressure ratio P3/P2	-

Greek letters

η_o	Engine efficiency	-
ε	Mass fraction	-
φ	Relative humidity	-

Subscript

ad	Adapted engine configuration
Amb	Ambient
cruise	Cruise
ISA	International standard atmosphere
ref	Reference engine configuration
C	Critical
D	Partial pressure of water vapour
F	Fuel
p	Exhaust plume

Thermodynamic stations

0	Free stream air conditions
2	First compressor front face
3	Last compressor discharge or burner entrance
4	Burner discharge, high-pressure turbine entrance
45	High-pressure turbine exit, low-pressure turbine entrance
5	Low-pressure turbine exit
7	Engine/exhaust nozzle interface
8	Exhaust nozzle throat

Abbreviations

AIC	Aircraft-induced cloudiness
HPT	High-pressure turbine
LH2	Liquid hydrogen
LPT	Low-pressure turbine
RF	Radiative forcing
RH	Relative humidity
SAC	Schmidt-Appleman criterion
SFC	Specific fuel consumption

1 Introduction

Contrails are thin, elongated clouds in the atmosphere, typically generated by aircraft flying in the upper troposphere or lower stratosphere at altitudes between 8 and 13 km [1]. Contrail research began in the early twentieth century. Thermodynamical theories on contrail formation were developed by Schmidt and Appleman who published their work in 1941 and 1953, respectively [2, 3]. These theories were further expanded and validated in flight tests by Schumann [4, 5]. In general, contrails can form when engine exhaust gases mix with ambient air. Water condenses on exhaust particles and atmospheric particles already present in the ambient air, which act as condensation nuclei. Due to the low temperatures at high altitudes, these water droplets quickly freeze, forming visible contrails. According to the Schmidt-Appleman criterion, which is described in Sect. 2, the ambient temperature and the temperature and water vapour content of the exhaust gases are the main factors that determine whether this occurs. In reality, the physics of contrail formation is highly complex and also depends on the properties of the exhaust particles and the dynamics of the nucleation of the ice. [6, 7] In a dry environment, contrails usually dissipate within minutes after forming. In air supersaturated with respect to ice, contrails do not dissipate as quickly and can remain in the atmosphere for hours. These long-lasting contrails are referred to as persistent contrails, which can begin to grow and evolve into cirrus clouds [4, 8]. These clouds remain in the upper troposphere, reflecting long-wavelength radiation back to Earth, and thereby contribute to the greenhouse effect through radiative forcing (RF).

However, persistent contrails can also induce a cooling effect by reflecting incoming short-wave solar radiation back into space, which is known as the albedo effect [8]. These effects counteract each other and depend highly on the geographic location, altitude, year, and time of day, as well as atmospheric state [9]. While net-negative RF does occur in the above mentioned instances [10], the calculated contrail-induced RF effect generally presents as net positive. This contributes to anthropogenic climate change [11]. Furthermore, satellite data suggest that the real contrail long-wavelength RF is much larger than the theoretical calculated RF, further increasing the warming effect [12].

Contrails can be avoided by operational and technical means. One operational approach to reduce climate-relevant contrails is to detect the areas where persistent contrails can form and then bypassing these by means of flight altitude changes or flight route adjustments. This has been investigated by Mannstein et al. [13], who found that minor flight altitude adjustments can prevent a large fraction of contrails and aircraft-induced cloudiness. The main hurdles for this approach are airspace integration and the detection of atmospheric layers where persistent contrails form. These hurdles are avoided if the contrails are prevented where they originate, at the engine itself, by technical contrail suppression.

Technical contrail suppression deals with the design and operation of the aircraft engine, as well as the fuel used. There are three main approaches: reducing the amount of water in the exhaust gas by using hydrogen-poor fuels or removing water from the exhaust; reducing particulate emissions, thus also reducing the amount of condensation nuclei; and increasing the exhaust temperature so that the exhaust plume can mix more thoroughly with the dry environment before condensation occurs. [9]

One option is to reduce the fuel's water emission index, which denotes the mass of water produced per mass of

fuel burned. However, the possibilities are relatively limited because the properties of jet fuels are subject to strict rules. Another option is to increase the heating value of the fuel. The fraction of the water emission index divided by the heating value is the energy-specific emission index. This index is larger for alternative fuels, such as methane and liquid hydrogen (LH2), than for kerosene. Gierens et al. [9] found that aircraft operating with these alternative fuels produce contrails at lower altitudes than aircraft operating with conventional kerosene.

Noppel et al. [14] proposed the water-enhanced turbofan (WET) concept with heat exchangers placed in the engine bypass and core. These cool the exhaust gas and condense the water vapour. The condensate is captured, along with a significant amount of the otherwise released soot particles [15]. Gao et al. [16] found that contrail formation is prevented when 70 % of the produced water is removed from the exhaust gases of a LEAP 1-A engine during cruise at 35 000 feet by condensation via a heat exchanger. The condensate runs out of the engine and will drop to a lower and warmer altitude due to the large droplet size.

Instead of removing water from the exhaust gases, another option is to reduce the condensation nuclei present. Gierens [17] proposed that certain fuel additives can reduce the condensation potential of the emitted particles. Similarly, Burkhardt et al. [6] found that reducing engine soot emissions shortens the contrail cirrus lifespan, as well as reducing their optical depth. Exhaust particle formation can also be suppressed by employing alternative fuels, like sustainable aviation fuels (SAFs) or LH2 [18]. Narciso et al. [19] found that contrails produced by alternative fuels have lower optical densities and lifespans than conventional contrails, reducing their climate impact.

While the above studies highlight the potential of alternative fuels and advanced engine cycles for contrail avoidance, significant challenges, like the introduction of heat exchangers, remain that prevent their widespread implementation in the near term. Therefore, we focus on an alternative approach in this paper: temporarily increasing the exhaust gas temperature to inhibit contrail formation using existing technologies that can be deployed relatively quickly. Exhaust temperature is increased by decreasing the overall efficiency of the aircraft engine and there are various ways to do this. The challenge is to raise the exhaust temperature as much as possible without exceeding the engine's operating limits. Little work has been published on this topic.

Haglind [20] found that employing variable guide vanes (VGVs) in the fan can reduce the contrail formation threshold temperature by 1.5 K. This translates to a decrease in engine efficiency of up to 11 % for the engine he studied. This decrease corresponds to a critical altitude increase of about 300 m in the troposphere. However, the specific fuel consumption (SFC) is also increased by up to 45 %, depending on altitude.

To the best of our knowledge, there are no published investigations on other technical means at the engine level. Therefore, we explore the idea of influencing the engine efficiency to mitigate contrail formation further in this paper. For this, we select a typical flight and aircraft configuration. According to Wilkerson [21], short- and medium-range air traffic makes up 96 % of the total air traffic volume. Accordingly, the selected engine model is representative of a typical engine utilized in the short- to medium-range aircraft class (Airbus A320neo). The analyzed operating point is cruise flight.

2 Theory

In this section, the thermodynamic theory used to describe contrail formation is outlined. During flight, the gas turbine engine emits a jet of exhaust gas consisting of heated air and combustion products that rapidly mixes with the surrounding atmosphere. The mixing process is described in thermodynamic terms based on the conservation of mass and energy. An in-depth dicussion of the SAC can be found in Schumann 1996 [4].

According to the SAC, contrails form if the exhaust plume-air mixture reaches saturation with respect to water during the mixing process. Saturation is reached when the relative humidity RH, which is a function of temperature, reaches 100 %.

In Fig. 1, two such mixing lines of the exhaust gasses with the ambient air are plotted in a diagram showing the

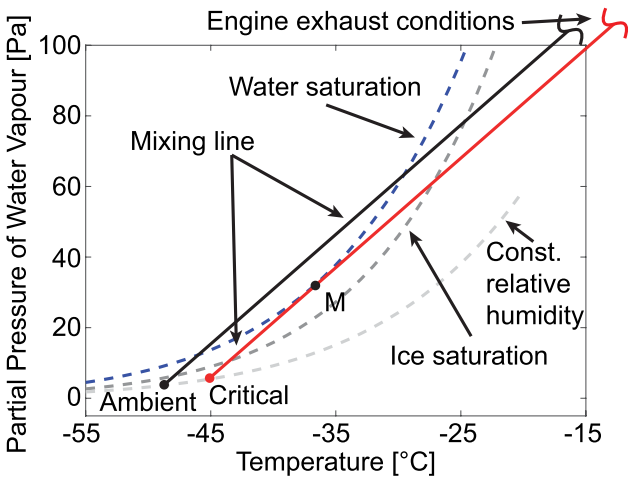

Fig. 1 Partial pressure of water vapour vs. temperature graph, derived from Schumann [5]. The red mixing line is chosen so that contrails just begin to form at point M for a critical ambient temperature at point C. Persistent contrails form if the ambient conditions are above the ice saturation line

relationship between partial pressure of water vapour and temperature. Under the assumptions of ideal mixing, constant specific heat capacity, isobaric conditions, and no phase change and therefore no latent heat release, the mixing line is a straight line that connects the engine exhaust conditions above and to the right of the graph with the ambient temperature and partial pressure of water vapour in the bottom left. If the mixing line touches the water saturation line at point M, contrails will just begin to form. Hence, contrails will form at any ambient temperature T_{Amb} colder than the critical ambient temperature T_C for mixing lines with the same slope G.

As shown in Fig. 1, the slope G is a critical parameter in determining whether contrails will form. Schumann [4] proposed to calculate the slope G of the mixing line with

$$G = \frac{\Delta P_D}{\Delta T} = \frac{\mathrm{EI_{H2O}}\, P_{s,\mathrm{Amb}}\, C_p}{\epsilon\, \mathrm{FHV}\, (1-\eta_o)}, \tag{1}$$

with the fuel's water emission index $\mathrm{EI_{H20}}$, which denotes the mass of water produced per mass of fuel burned. $\mathrm{EI_{H20}}$ is given in $\mathrm{kg_{water}/kg_{fuel}}$. $P_{s,\mathrm{Amb}}$ is the static ambient pressure and C_p the specific heat capacity in the plume. ϵ is the molar mass fraction of water to dry air, given as $\epsilon = 0.622$. FHV is the fuel heating value of the fuel and η_o the overall engine efficiency. The engine efficiency can be expressed as

$$\eta_o = \frac{F_N\, V_0}{W_F\, \mathrm{FHV}}\,. \tag{2}$$

The temperature at point M in Fig. 1 is at the point where

$$\frac{\mathrm{d}P_D}{\mathrm{d}T} = G\,. \tag{3}$$

The critical temperature is defined as the ambient temperature at which contrails will just begin to form for a given engine efficiency and flight conditions.

The mixing line slope G increases with engine efficiency, thus also increasing T_M and T_C. Therefore, more efficient engines cause contrails at higher ambient temperatures and lower altitudes due to the increased relative humidity in their colder plumes.

In order to decrease the mixing line's slope, the engine efficiency has to be reduced, as previously shown by Haglind [20]. The goal is to decrease the mixing line slope to such a degree that the mixing line does not cross the water saturation line in the partial pressure of water vapour vs. temperature diagram, as shown in Fig. 2

Mathematically, this condition can be tested for with the critical temperature. The critical temperature can also be converted into a critical altitude ALT_C, which is valid for a given engine configuration and flight condition. The critical altitude therefore denotes the altitude at which an aircraft will produce contrails for a given engine efficiency and

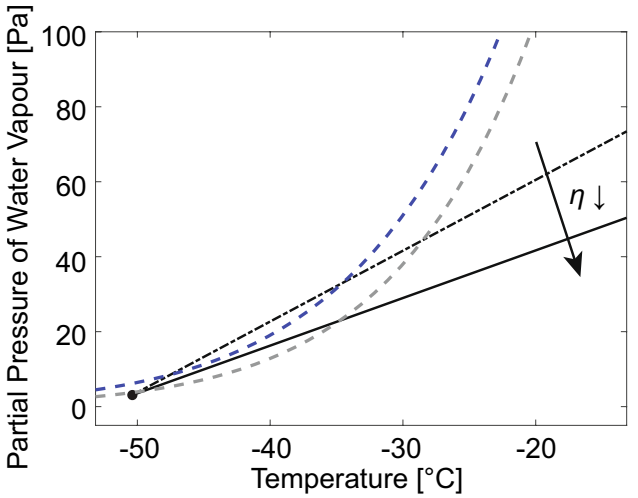

Fig. 2 Influence of the engine efficiency on the mixing line slope. The goal is to decrease the engine efficiency enough so that the new mixing line (solid black) does not touch or cross the water saturation line (blue dashed)

cruise speed. We employ the increase or decrease in critical altitude after an engine design or operating point adjustment as a metric that is used to evaluate the proposed change. The change in critical altitude is calculated as

$$\Delta\mathrm{ALT}_C = (T_{C,\mathrm{ref}} - T_{C,\mathrm{ad}})\, \frac{1000\,\mathrm{m}}{6.5\,\mathrm{K}}\,, \tag{4}$$

with 6.5 K the rate of temperature decrease per 1000 m of altitude in the troposphere [22].

This critical altitude difference $\Delta\mathrm{ALT}_C$ is shown in Fig. 3 with the standard temperature shown in red where contrails will form and blue where contrails will not form.

Furthermore, the increase in SFC is used as an additional metric, representing the adverse operational effect for the gain in critical altitude.

3 Method

In this section, the cruise conditions and thrust requirements are outlined first. Second, the reference engine configuration and design point are discussed. Third, the study design and examined engine parameters are introduced, followed by the implementation of the SAC.

3.1 Cruise conditions and thermodynamic engine model

The selected typical flight and aircraft configuration are those of the short- to medium-haul aircraft class. Contrails typically occur in cruise; therefore, this operating point is

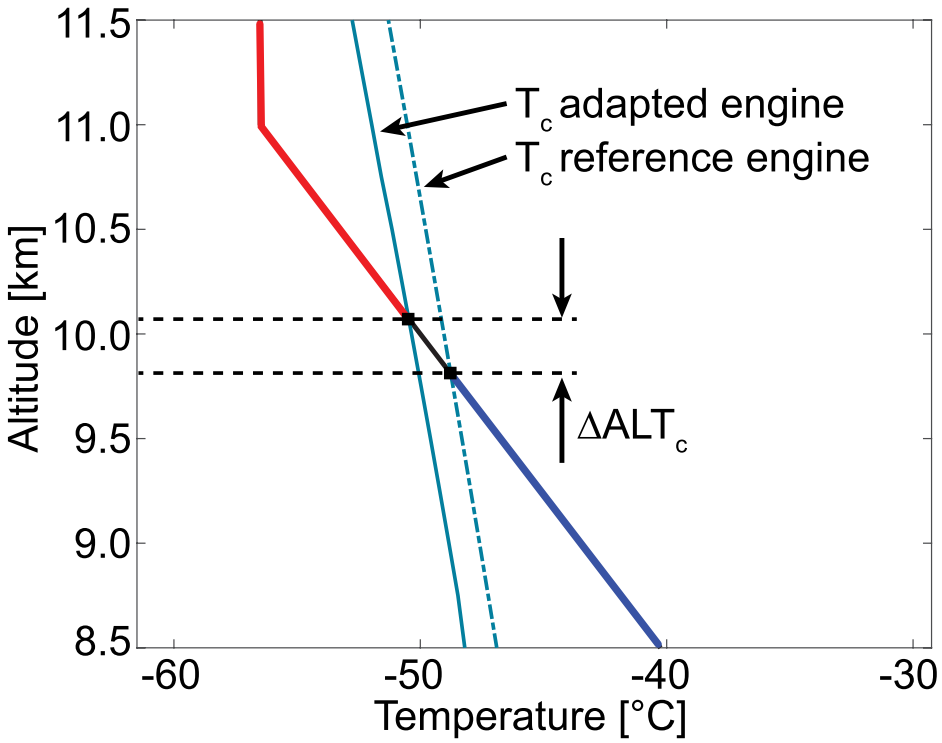

Fig. 3 Critical altitude difference as calculated from the critical temperature. Where the ISA temperature [22] line is shown in red, contrails will form. The goal of decreasing the engine efficiency is to achieve a ΔALT_c large enough to shift the intersection between the critical temperature line and the ISA-temperature line above the cruise altitude, inhibiting contrail formation

Table 1 Engine parameters

Engine parameter	Value
Overall pressure ratio	32.3
Burner Exit Temperature	1350 K
Design bypass ratio	12
Net cruise thrust	18.7 kN
SFC	14.51 g/(kNs)
Static sea level net thrust	120 kN

Table 2 Upper and lower limits of the examined parameters

Parameter	Lower [%]	Upper [%]
Core nozzle area	−45	+45
Bypass nozzle area	−40	+40
HPT capacity	−35	+35
LPT capacity	−15	+20
Handling bleed	0	20
High-pressure bleed	0	10

examined. It should be noted, however, that contrails can occur at any altitude, depending on ambient conditions.

The required net thrust in cruise is set at $F_N = 18.7\,\text{kN}$ per engine, at an altitude of $ALT_0 = 10\,058\,\text{m}$ and a Mach number of $M_0 = 0.78$. These values represent typical cruise parameters of an Airbus A320neo. The thrust requirement needs to be fulfilled for all parameter adjustments to maintain the cruise speed and altitude.

GasTurb 14 [23–26] is used to model a typical geared turbofan engine of the A320neo. The engine design parameters are listed in Tab. 1.

3.2 Study design

The examined engine parameters are varied with the aim to reduce the overall efficiency of the engine. The parameters and the applied limits of the study are given in Tab. 2. The high-pressure and low-pressure turbine (HPT and LPT) capacities are decreased by reducing the turbine entry cross-section. The parameter limits are selected in a manner that ensures the thermodynamic engine cycle remains stable and the operational parameters remain within their critical limits. The engine operating limits are given in

Table 3 Engine limits

Engine parameter	Limit
Burner exit temperature	1650 K
HPC spool speed	104 %

Tab. 3. The cruise thrust needs to be maintained to uphold the cruise speed of $M_0 = 0.78$.

The effect of the parameter variation on contrail formation is then examined by means of the difference in critical altitude between the reference and adapted engine models.

Lastly, the effect on the engine turbine temperatures and the overall pressure ratio (OPR) is quantified. Here, T_4 is the HPT entry temperature, T_{45} the LPT entry temperature, and T_5 the LPT exit temperature. For the most promising adaptations, the altitude-temperature Schmidt-Appleman diagram is shown under the assumption of constant engine efficiency and thrust. The altitude range where these assumptions are valid is between 8 500 and 11 500 m.

The parameter studies are conducted using batch jobs in GasTurb to vary the engine parameters. The results were then exported and post-processed in MATLAB.

The ambient humidity is altered between 0 % and 100 % in 25 % increments.

To contextualise the results, the critical altitude for the chosen engine configuration and cruise parameters is 9.6 km at 50 % ambient humidity. Therefore, the critical altitude increase required to prevent contrails at cruise altitude for 50 % ambient humidity would need to exceed 450 m.

3.3 Implementation of the SAC

The SAC was implemented in MATLAB. GasTurb is used to calculate the engine parameters needed for the SAC. These are then imported into MATLAB for further processing using the equations outlined in Sect. 2.

The water and ice saturation vapour pressure curves are calculated using the formulas outlined in the CIMO 2023 report [27, 28].

The critical temperature is evaluated for a given ambient humidity with a Newton-iteration.

Table 4 Delta T_C and $\Delta\mathrm{ALT}_C$ for the examined parameters at 50 % humidity

Parameter	Δ [%]	ΔT_C [K]	$\Delta\mathrm{ALT}_C$ [m]
Core nozzle area	−45	0.91	140
Bypass nozzle area	+40	1.34	206
HPT capacity	+35	0.64	98
LPT capacity	−15	0.37	57
Handling bleed	20	0.38	58
High-pressure bleed	10	0.51	79

4 Results

In this section, the study results are presented. Table 4 provides an overview of the possible critical temperature change for 50 % humidity with regard to the six parameters taken into account. According to the SAC, persistent contrails only form at relative humidities with regards to water of greater than around 59 %. At 59 % RH, the air is ice-saturated. Therefore 50 % was chosen as a lower humidity boundary, given the 25 % increment in humidity used for the study. The resulting altitude difference at which contrails will begin to form was calculated according to equation (4). In general, the larger the gain in critical altitude $\Delta\mathrm{ALT}_C$, the better.

4.1 Core nozzle area

Decreasing the core nozzle area by 45 % achieved a maximum critical altitude increase of $\Delta\mathrm{ALT}_C = 140$ m. The corresponding critical temperature change was 0.91 K. Figure 4 shows the Schmidt-Appleman altitude-temperature diagram for the most effective core nozzle area change of −45 %.

At the given cruise conditions with an altitude of 10 058 m, altering the core nozzle area was unable to prevent contrails from forming above 0 % humidity. As illustrated in Fig. 4, the intersection between the ISA temperature line and the adjusted critical temperature line is situated below the cruise altitude for ambient relative humidity greater than 0 %. To the left of the 0 % relative humidity line, contrails will always form. Contrails cannot form to the right of the 100 % line. In the area between these lines, contrails can form.

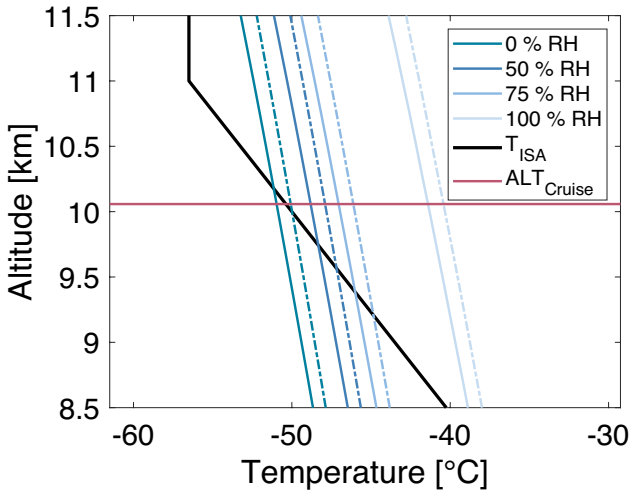

Fig. 4 Altitude-temperature SAC-graph for 45 % decreased core nozzle area for constant η_o plotted as a function of altitude. The dash-dotted lines represent the reference engine configuration, the solid the adapted engine configuration for the given ambient relative humidity (RH). The black line represents the ISA-temperature

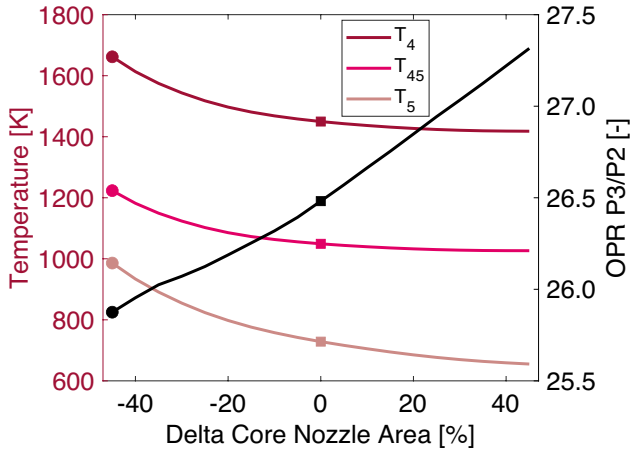

Fig. 5 Influence of the core nozzle area change on turbine temperatures and the OPR for 50 % humidity. T_4 is the HPT entry temperature, T_{45} the HPT exit or LPT entry tempreature and T_5 is the LPT exit temperature. The circles denote the highest achieved ΔALT_c

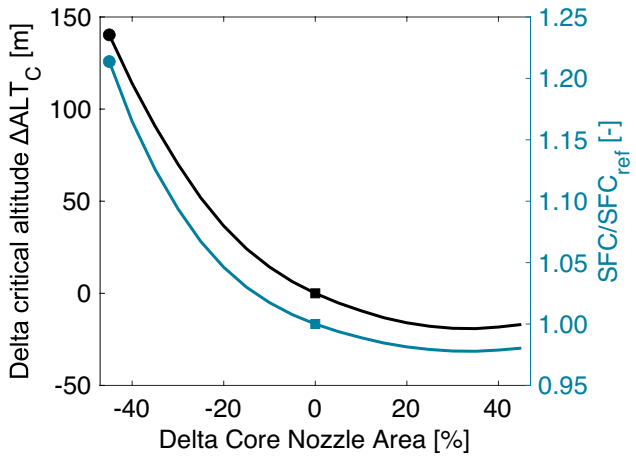

Fig. 6 Influence of the core nozzle area on the achievable critical altitude increase ΔALT_c and the SFC for 50 % humidity

Hence, contrails still formed during cruise. Furthermore, the 140 m critical altitude gain corresponded to a 23 % increase in SFC. The influence of the core nozzle area variation on the turbine temperatures, OPR and SFC is shown in Fig. 5 and Fig. 6, respectively.

T_5 increased by 250 K, while T_4 and T_{45} increased by approximately 200 K. Reducing the core nozzle area decreased the power delivery of the turbines, which was compensated for by increased fuel flow. The overall pressure ratio has a linear relationship to the core nozzle area, but remained largely unaffected, deviating by less than 4 % from the reference configuration.

Lastly, the critical altitude change ΔALT_C and the relative change in SFC are plotted over the adapted core nozzle area for a given humidity in Fig. 6.

A linear relationship between the increase in critical altitude and the increase in SFC can be observed.

Only a nozzle area decrease was identified as a viable option. Increasing the core nozzle area had no discernible effect on the critical altitude. It should also be noted that the ambient humidity had very little effect on the change in critical temperature and altitude. The main influence of the ambient humidity was the critical altitude itself, as can be seen in Fig. 4 by the intersection between the relative humidities and the ISA-temperature line.

4.2 Bypass nozzle area

Figure 7 shows the mixing line for the highest critical altitude difference in this study, achieved by increasing the bypass nozzle area by 40 %.

The resulting critical temperature difference of 1.34 K increased the critical altitude by 206 m. Despite that, the mixing line still crosses the water saturation curve. At lower ambient humidity, the mixing line remains below the water saturation line, preventing contrails from forming.

Figure 8 shows the critical temperature change as a function of the cruise altitude.

Similarly to the results in Fig. 4, in Fig. 8 the adapted critical temperature lines cross the ISA temperature line below the cruise altitude for ambient humidity greater than 50 %.

The influence of the bypass nozzle change on the turbine temperatures and the OPR is shown in Fig. 9. Changing the bypass nozzle area increased the turbine temperatures slightly more than 8 %.

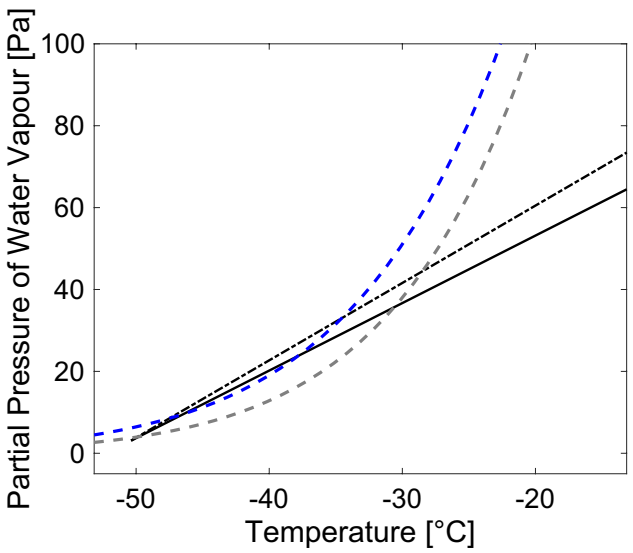

Fig. 7 Mixing line for a bypass nozzle area increase of 40 %. The solid black is the adapted engine configuration. It crosses the water saturation line (blue dashed), enabling contrails to form

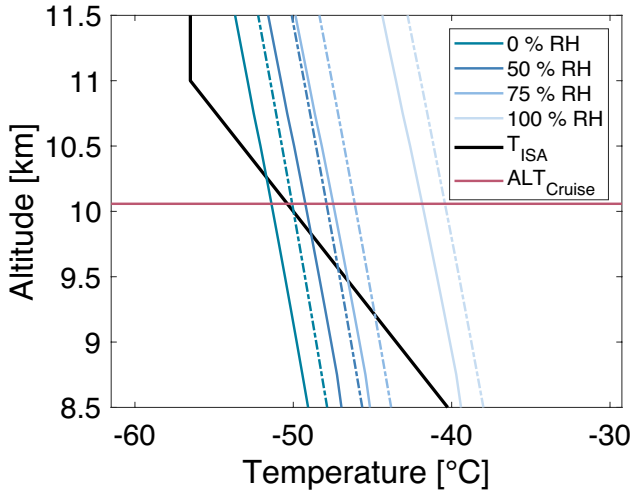

Fig. 8 Altitude-temperature SAC-graph for 40 % increased bypass nozzle area for constant η_o. The dash-dotted lines represent the reference engine configuration, the solid the adapted engine configuration. The black line is the ISA-temperature

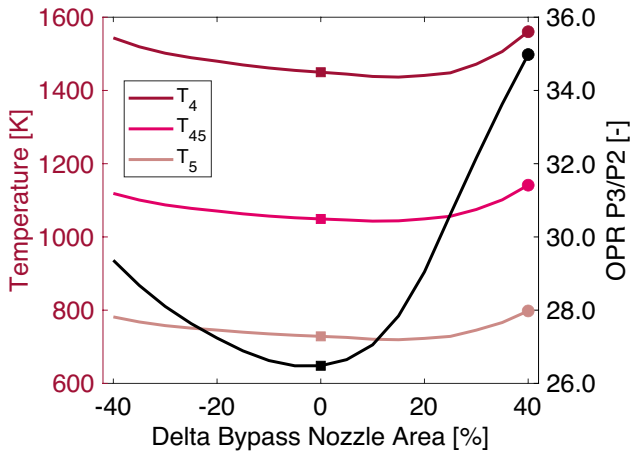

Fig. 9 Influence of the bypass nozzle area change on turbine temperatures and the OPR for 50 % humidity. T_4 is the HPT entry temperature, T_{45} the HPT exit or LPT entry tempreature and T_5 is the LPT exit temperature. The circles denote the highest achieved ΔALT_c

Increasing the bypass nozzle area also increased the power demand of the turbine stages, increasing fuel consumption. The OPR increased to a maximum of 35, while the core thrust increased and exceeded the bypass thrust. Here, surging could occur in the booster stage, requiring a mitigation strategy. Figure 10 illustrates the achievable increase in critical altitude and its impact on SFC. As with the previous case, the altitude change correlated closely with the change in SFC and therefore the increased fuel burn. At +40 % bypass nozzle area and an achieved 206 m altitude difference, the SFC increased by 35 %.

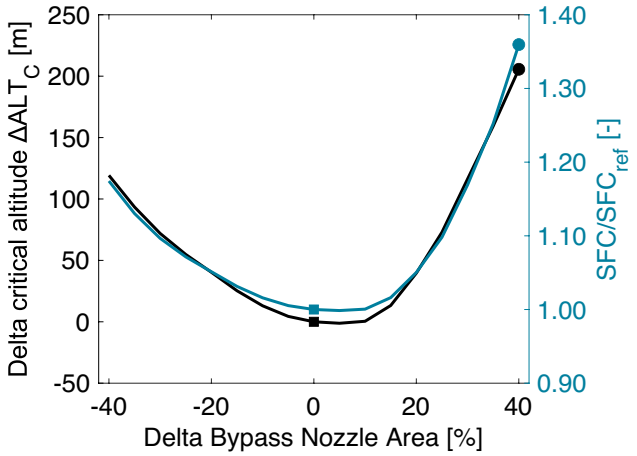

Fig. 10 Influence of the bypass nozzle area on the achievable critical altitude increase ΔALT_c and the SFC for 50 % humidity

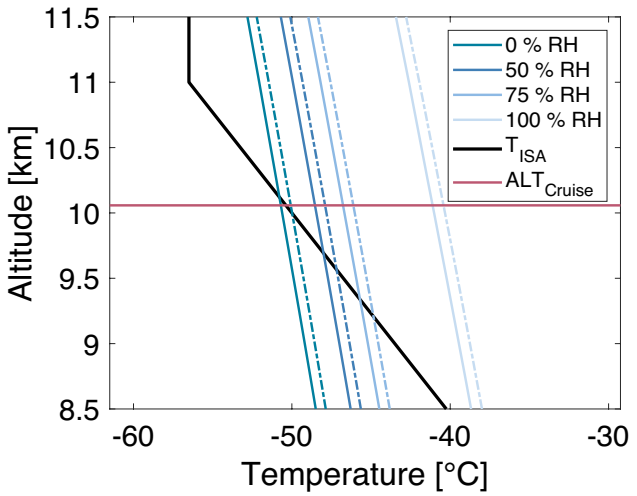

Fig. 11 Altitude-temperature SAC-graph for 35 % increased HPT capacity for constant η_o. The dash-dotted lines represent the reference engine configuration, the solid the adapted engine configuration. The black line is the ISA-temperature

It was possible to achieve a critical altitude increase through a reduction or an increase in the area of the bypass nozzle. However, increasing the bypass nozzle area had the higher critical altitude potential.

4.3 High-pressure turbine capacity

Of the three most promising engine parameters, the HPT capacity showed the least potential, while also being the most technically challenging engine adaptation to implement. A change of +35 % increased the critical temperature by 0.64 K, resulting in a critical altitude increase of 98 m. The distance between the reference critical temperature lines

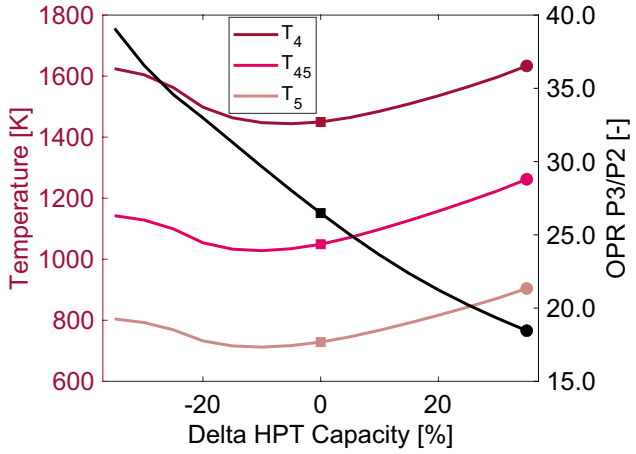

Fig. 12 Influence of the HPT capacity change on turbine temperatures and the OPR for 50 % humidity. T_4 is the HPT entry temperature, T_{45} the HPT exit or LPT entry tempreature and T_5 is the LPT exit temperature. The circles denote the highest achieved ΔALT_c

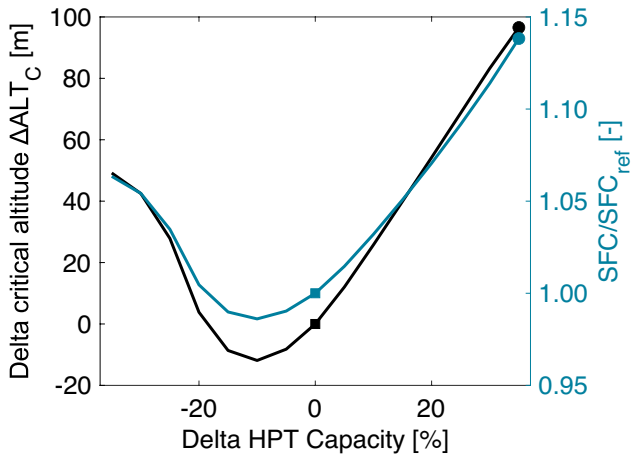

Fig. 13 Influence of the HPT capacity on the achievable critical altitude increase ΔALT_c and the SFC for 50 % humidity

(dash-dotted) and the adapted engine configuration (solid) in Fig. 11 decreased further in comparison to the nozzle areas.

The temperature influence, OPR, and SFC are shown in Fig. 12 and Fig. 13.

The turbine temperatures T_4, T_{45}, and T_5 increased by 13 %, 21 %, and 24 %, respectively. This equated to a roughly 200 K increase in turbine entry temperatures for the LPT and HPT. The overall pressure ratio decreased with increased HPT capacity. This is due to surging in the booster stage, requiring mitigation via handling bleeds or inlet guide vanes (IGVs). Again, the SFC and the critical altitude difference showed similar trends. At a critical altitude increase of 98 m, the SFC was observed to be 14 % higher in comparison to the reference engine.

4.4 LPT capacity, handling bleed, and high-pressure bleed

Among the three remaining examined adaptions, increasing the high-pressure bleed had the greatest effect, raising the critical altitude by 79 m, followed by the handling bleed (58 m), and the LPT capacity (56 m). This increase was accompanied by an increase in SFC of 11 %, 8 %, and 7 %, respectively. With all three adaptions the power delivery of the turbines decreased, which was compensated for by an increase in fuel consumption. This resulted in an increase in waste heat within the engine cycle, decreasing the engine efficiency. The critical altitude and SFC over engine parameter figures for these are presented in appendix A, B, and C (Figs. 14, 15, 16, 17, 18, 19).

As a further option to decrease the engine efficiency, the variable guide vanes (VGVs) in the compressor stages could be utilised. These are implemented in most engines and therefore readily available. However, closing the VGVs in the booster stage increased the critical altitude by around 40 m, while increasing the SFC by 6 %. A similar adjustment in the HPC increased the critical altitude by merely 10 m, while increasing the fuel consumption by 2 %. Higher critical altitude changes were not achievable as the required cruise thrust could not be maintained if the VGVs were closed further.

5 Discussion and outlook

Engine design and operating point adaptations have the potential to increase the critical altitude at which contrails begin to form for a given engine configuration and cruise speed. The resulting increase in critical altitude is insufficient to prevent persistent contrails from forming at a cruising altitude of 10 058 m for ambient humidity with respect to water of greater than 50 % and we find that preventing or avoiding this type of contrail is not possible with the proposed engine changes.

The maximum critical altitude increase achieved, regardless of ambient humidity, is just over 200 m with a bypass nozzle area increase of 40 %. This correlates with an increase in SFC of 36 % and up to 125 K higher turbine temperatures, which in turn decreases the engine lifespan without achieving the goal of preventing persistent contrails. To achieve this goal, the critical altitude would have to increase by more than 450 m. All data is provided in full in the method and results section of this paper.

Operational contrail prevention measures appear to be a more viable alternative to reduce the climate-impact caused by the aviation industry. However, the calculations presented

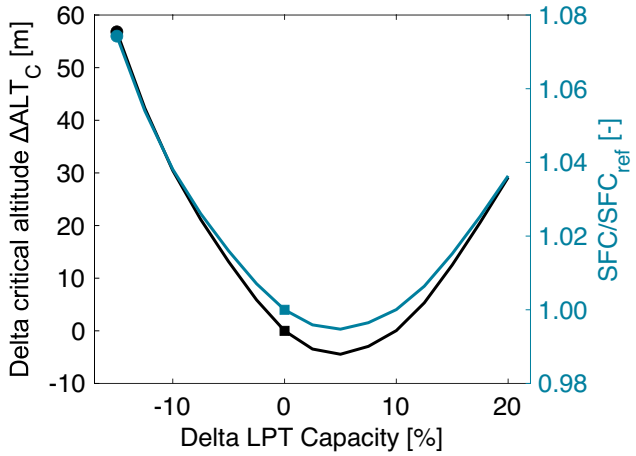

Fig. 14 Influence of the LPT capacity on the achievable critical altitude increase ΔALT_c and the SFC for 50 % humidity

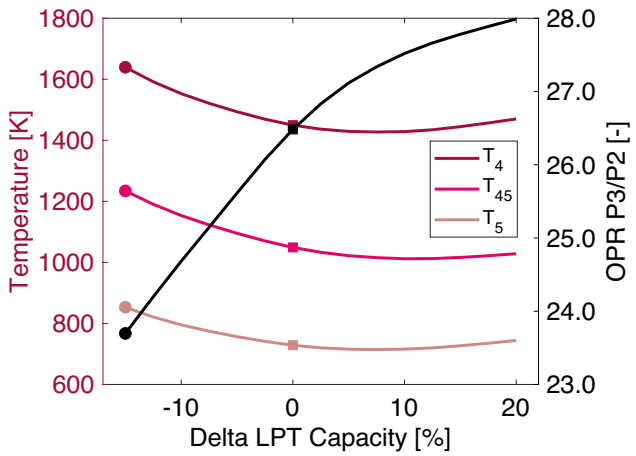

Fig. 15 Influence of the HPT capacity change on turbine temperatures and the OPR for 50 % humidity. T_4 is the HPT entry temperature, T_{45} the HPT exit or LPT entry tempreature and T_5 is the LPT exit temperature. The circles denote the highest achieved ΔALT_c

here can be used to predict when contrails will start to form in preliminary engine design studies.

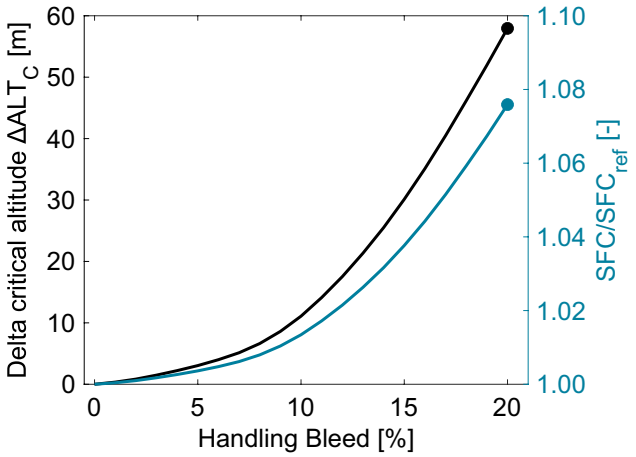

Fig. 16 Influence of the handling bleed on the achievable critical altitude increase ΔALT_c and the SFC for 50 % humidity

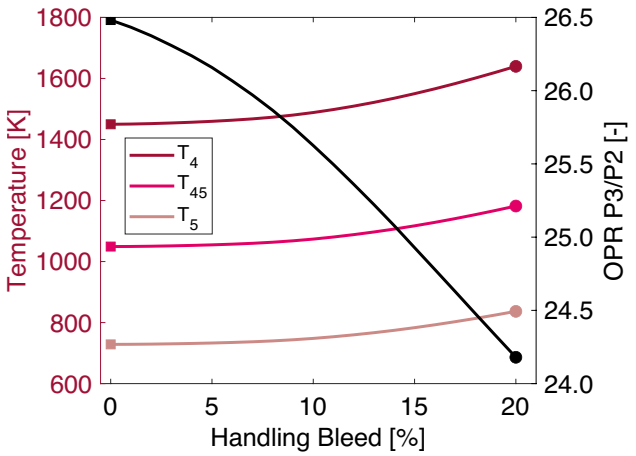

Fig. 17 Influence of the handling bleed change on turbine temperatures and the OPR for 50 % humidity. T_4 is the HPT entry temperature, T_{45} the HPT exit or LPT entry tempreature and T_5 is the LPT exit temperature. The circles denote the highest achieved ΔALT_c

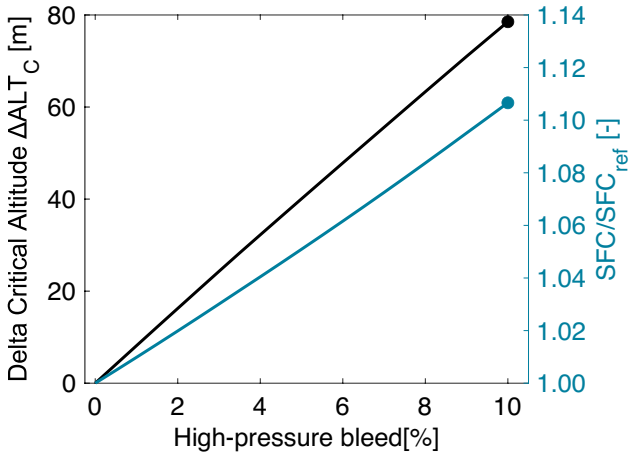

Fig. 18 Influence of the high-pressure bleed on the achievable critical altitude increase ΔALT_c and the SFC for 50 % humidity

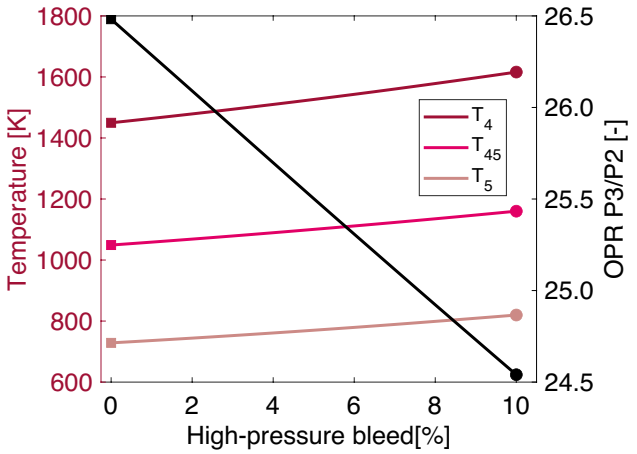

Fig. 19 Influence of the high-pressure bleed change on turbine temperatures and the OPR for 50 % humidity. T_4 is the HPT entry temperature, T_{45} the HPT exit or LPT entry tempreature and T_5 is the LPT exit temperature. The circles denote the highest achieved ΔALT_c

The calculations can be repeated for different engine types. However, the outcome is expected to diverge only marginally from the results obtained by the authors. Future work could concentrate on the development of contrail prediction methods based on performance calculations in accordance with the Schmidt-Appleman criterion, with the objective of establishing a reliable methodology for forecasting contrail formation during flight. This would enable operational measures like climbing above or below critical, ice-supersaturated atmospheric layers to avoid persistent contrails to be utilised.

Appendix A: LPT capacity

See Figs. 14, 15 here.

Appendix B: Handling bleed

See Figs. 16, 17 here.

Appendix C: High-pressure bleed

See Figs. 18, 19 here.

Funding Open Access funding enabled and organized by Projekt DEAL.

Data availability All data is provided in full in the results section of the paper. I will add the required statement in the conclusion

Open Access This article is licensed under a Creative Commons Attribution 4.0 International License, which permits use, sharing, adaptation, distribution and reproduction in any medium or format, as long as you give appropriate credit to the original author(s) and the source, provide a link to the Creative Commons licence, and indicate if changes were made. The images or other third party material in this article are included in the article's Creative Commons licence, unless indicated otherwise in a credit line to the material. If material is not included in the article's Creative Commons licence and your intended use is not permitted by statutory regulation or exceeds the permitted use, you will need to obtain permission directly from the copyright holder. To view a copy of this licence, visit http://creativecommons.org/licenses/by/4.0/.

Conflict of interest The authors declare no competing interests.

References

1. Kärcher, B.: Formation and radiative forcing of contrail cirrus. Nat. Commun. **9**(1), 2018 (1824). https://doi.org/10.1038/s41467-018-04068-0
2. Schmidt, E.: Die entstehung von eisnebel aus den auspuffgasen von flugmotoren. Schiften der Deutschen Akademie der Luftfahrtforschung **44**(5), (1941)
3. Appleman, H.: The formation of exhaust condensation trails by jet aircraft. Bullet. Am. Meteorol. Soc. **34**(1), 14–20 (1953)
4. Schumann, U.: On conditions for contrail formation from aircraft exhausts. Meteorol. Z. **5**(1), 4–23 (1996)
5. Schumann, U.: Influence of propulsion efficiency on contrail formation. Aerosp. Sci. Technol. **4**, 391–401 (2000)
6. Burkhardt, U., Bock, L., Bier, A.: Mitigating the contrail cirrus climate impact by reducing aircraft soot number emissions. npj Climate Atmos. Sci. (2018). https://doi.org/10.1038/s41612-018-0046-4
7. ...Voigt, C., Kleine, J., Sauer, D., Moore, R.H., Bräuer, T., Le Clercq, P., Kaufmann, S., Scheibe, M., Jurkat-Witschas, T., Aigner, M., Bauder, U., Boose, Y., Borrmann, S., Crosbie, E., Diskin, G.S., DiGangi, J., Hahn, V., Heckl, C., Huber, F., Nowak, J.B., Rapp, M., Rauch, B., Robinson, C., Schripp, T., Shook, M., Winstead, E., Ziemba, L., Schlager, H., Anderson, B.E.: Cleaner burning aviation fuels can reduce contrail cloudiness. Commun. Earth Environ. (2021). https://doi.org/10.1038/s43247-021-00174-y
8. Schumann, U.: Formation, properties and climatic effects of contrails. C R Phys. **6**, 549–565 (2005)
9. Gierens, K., Lim, L., Eleftheratos, K.: A review of various strategies for contrail avoidance. The Open Atmos. Sci. J. **2**, 1–7 (2008)

10. Meyer, R., Mannstein, H., Meerkötter, R., Schumann, U., Wendling, P.: Regional radiative forcing by line-shaped contrails derived from satellite data. J. Geophys. Res.: Atmos. **107**(D10), ACL 17-1-ACL 17-15 (2002). https://doi.org/10.1029/2001JD000426
11. Meerkötter, R., Schumann, U., Doelling, D.R., Minnis, P., Nakajima, T., Tsushima, Y.: Radiative forcing by contrails. Ann. Geophys. **17**(8), 1080–1094 (1999). https://doi.org/10.1007/s00585-999-1080-7
12. Minnis, P., Palikonda, R., Walter, B.J., Ayers, J.K., Mannstein, H.: Contrail properties over the eastern north pacific from avhrr data. Meteorol. Z. **14**, 515–523 (2005)
13. Mannstein, H., Spichtinger, P., Gierens, K.: A note on how to avoid contrail cirrus. Transp. Res. Part D: Transp. Environ. **10**(5), 421–426 (2005). https://doi.org/10.1016/j.trd.2005.04.012
14. Noppel, F., Singh, R., Taylor, M.: Novel engine concept to suppress contrail and cirrus cloud formation. Precedings of the TAC-Conference, pp. 221–240 (2006)
15. Pouzolz, R., Schmitz, O., Klingels, H.: Evaluation of the climate impact reduction potential of the water-enhanced turbofan (wet) concept. Aerospace **8**(3), 59 (2021). https://doi.org/10.3390/aerospace8030059
16. Gao, X., Isoldi, A., Nalianda, D., Nikolaidis, T.: Water extraction in aero gas turbines for contrail mitigation. The Aeronautical Journal **128**(1325), 1344–1361 (2024). https://doi.org/10.1017/aer.2024.22
17. Gierens, K.: Are fuel additives a viable contrail mitigation option? Atmos. Environ. **41**(21), 4548–4552 (2007). https://doi.org/10.1016/j.atmosenv.2007.03.014
18. Williams, V.: The engineering options for mitigating the climate impacts of aviation. Philos. Transact. A Math. Phys. Eng. Sci. **365**(1861), 3047–3059 (2007). https://doi.org/10.1098/rsta.2007.0012
19. Narciso, M., de Sousa, J.M.M.: Influence of sustainable aviation fuels on the formation of contrails and their properties. Energies **14**(17), 5557 (2021). https://doi.org/10.3390/en14175557
20. Haglind, F.: Potential of lowering the contrail formation of aircraft exhausts by engine re-design. Aerosp. Sci. Technol. **12**(6), 490–497 (2008). https://doi.org/10.1016/j.ast.2007.12.001
21. Wilkerson, J.T., Jacobson, M.Z., Malwitz, A., Balasubramanian, S., Wayson, R., Fleming, G., Naiman, A.D., Lele, S.K.: Analysis of emission data from global commercial aviation: 2004 and 2006. Atmos. Chem. Phys. **10**, 6391–6408 (2010)
22. ICAO: Manual of the icao standard atmosphere: extended to 80 km (262 500 feet) - doc7488/3 (1993)
23. GasTurb GmbH. Gasturb 14, (2025)
24. Kurzke, J., Halliwell, I., Hill, R.: Propulsion and Power. Springer Nature Switzerland, Cham (2025). https://doi.org/10.1007/978-3-031-65026-0
25. Saravanamuttoo, H.I.H., Rogers, G.F.C., Cohen, H.: Gas Turbine Theory, 12th edn. Dorling Kindersley, India (2013)
26. Mattingly, J.D.: Elements of Gas Turbine Propulsion. Tata McGraw, New Delhi (2005)
27. Sonntag, D.: Fortschritte in der hygrometrie. Meteorol. Z. **3**(2), 51–66 (1994). https://doi.org/10.1127/metz/3/1994/51
28. World Meteorological Organization: Guide to Instruments and Methods of Observation: Volume I - Measurement of Meteorological Variables, volume Volume I. World Meteorological Organization, Geneva, wmo- no. 8 edition, 2023. (2023). ISBN 978-92-63-10008-5. URL https://library.wmo.int/records/item/68695-guide-to-instruments-and-methods-of-observation?language_id=13&back= &offset=4

Publisher's Note Springer Nature remains neutral with regard to jurisdictional claims in published maps and institutional affiliations.